Journal of Science and Technology – Engineering and Technology for Sustainable Development
Volume 36, Issue 1, March 2026, 001-008

Research on Chemically Modified Tire-Derived Char and Preliminary Evaluation of Activated Char/Mn-Co-CeO_x Catalysts for Toluene Treatment

Ta Dinh Quang[1], Khong Manh Hung[2], Tran Thi Thu Hien[3], Nguyen Thanh Hung[1], Nguyen Van Chuc[4], Le Minh Thang[1,*]

[1]*Hanoi University of Science and Technology, Ha Noi, Vietnam*
[2]*Institute of Chemistry and Materials, Vietnam Academy of Military Science and Technology, Ha Noi, Vietnam*
[3]*Faculty of Natural Sciences, Quy Nhon University, Binh Dinh Province, Vietnam*
[4]*Tech-Vina, Joint Stock Company, Hung Yen Province, Vietnam*
[*]*Corresponding author email: thang.leminh@hust.edu.vn*

Abstract

The study focuses on applying chemical agents to alter char obtained from the pyrolysis of rubber. The findings indicate that the collaborative using of potassium hydroxide (KOH) and HCl yields superior efficiency relative to their individual use. The carbon content in the modified char escalates from 69.9% to 85.5%, the BET-specific surface area experiences an approximate tripling (from 52 cm^2/g to 143 cm^2/g). Additionally, the mineral constituents, including Si, Ti, Ca, and Zn, as revealed by energy-dispersive X-ray spectroscopy (EDS) analysis, are markedly diminished, particularly Si, which declines from 6.4% to 0.8%. The EDS-Mapping analysis reveals a sparse distribution of the aforementioned metals following the modification process. The fourier transform infrared spectroscopy (FT-IR) analysis further substantiates that the vibrational intensity of the Si-O-Si bond is significantly diminished in the modified char sample, indicating its nearly complete removal. The capacity for toluene adsorption - desorption and oxidation performance of modified char also has been preliminarily evaluated and contrasted with that of activated carbon.

Keywords: Activated char, adsorption, Mn-Co-CeO_x, oxidation, rubber pyrolysis.

1. Introduction

Waste tire pyrolysis is a promising method of recycling, energy, and fuel recovery; it meets three solid waste treatment principles: reduction, resource recovery, and pollutant limitation [1]. The pyrolysis process degrades organic waste tire components, yielding gas products, oil condensate, and solid char. Therein, the char fraction is 22–49 wt%, whose economic value is a vital factor in determining the continued development of the commercialization of waste tire pyrolysisn processes [2]. In Vietnam, the Minh Tan Waste Treatment Plant in Hai Phong has mastered the technology of transforming waste tires into FO-R oil through pyrolysis. However, char products have not been fully utilized as modified to bring higher economic value. Beyond that, the studies [3], have indicated that activated char using physical and chemical agents can yield economically valuable carbon comparable to commercial activated carbon. This has led to significant research efforts to apply this modified carbon in various industrial sectors.

The physical activation method employs high-temperature steam CO_2, which often yields char with a tiny pore structure that is excellent for the adsorption of liquid and vapor phase chemicals [4]. Chemical carbon activation includes two methods: 1-step and 2-step activation. For 1-step activation, the pyrolysis and activation are performed at the same time, impregnating the precursor with chemical agents. Meanwhile, 2-step activation involves two processes. The first is the carbonization of the precursor, followed by the impregnating chemical agents to conduct activation [5]. This process is more flexible than physical activation because the surface porosity of activated carbon can be adjusted [6].

In recent years, potassium hydroxide (KOH) has often been widely used to produce low-cost activated carbon since KOH has the effect of dissolving SiO_2 theoretically and can increase the porosity of the material surface. According to research [7] carbon activation with KOH has better efficiency than activation with $ZnCl_2$ or H_3PO_4. Furthermore, KOH also significantly increases the specific surface area and the formation of -OH functional groups on the carbon surface [8]. In addition, some inorganic acids, such as HCl, HF, and H_2SO_4, are used as demineralization chemical agents to selectively remove impurities in pyrolysis char, including iron, zinc, sulfur, and silica. Lin *et al*. successfully removed silica using acid HF instead of HCl, which may result in the formation of a secondary product such as H_2SiF_6 [9]. Kurma *et al*. also investigated the removal of silica from char using a combination of HCl and HF. However, using large amounts of HF poses severe challenges to health and the environment on a larger scale. Furthermore, studies have

p-ISSN 3093-3242
e-ISSN 3093-3579
https://doi.org/10.51316/jst.188.etsd.2026.36.1.1
Received: Jan 23, 2025; Revised: May 7, 2025
Accepted: Aug 20, 2025; Online: Feb 5, 2026.

shown that HCl is more efficient than H_2SO_4 (93% by weight of carbon) [10]. As a result, HCl is regarded as the best chemical agent for modifying pyrolysis char when combined with KOH.

In brief, in this research, in order to activate the char from the rubber pyrolysis process and drastically reduce the mineral content to increase the carbon content in the char after modification, we will combine treatment with both KOH and HCl agents in the expectation of attaining char with beneficial properties. Then, the modified char will be employed as an adsorbent for volatile organic compounds (VOCs), especially toluen, serving as an effective approach for capturing hazardous substances. Additionally, volatile organic compounds can undergo treatment through oxidation facilitated by a transition metal oxide catalyst, transforming into less harmful byproducts like carbon dioxide and water. Our research group has developed a Mn-Co-CeO_x catalyst system exhibiting remarkable oxidation capacity [11].

In this study, we aim to integrate adsorption and oxidation techniques to fully address the treatment of the absorbed toluene. The adsorbent material is modified char derived from the rubber pyrolysis process, while the oxidized metal oxide system is based on the study team's findings. Following adsorption, toluene will experience concurrent desorption and oxidation processes. The levels of toluene throughout the adsorption and desorption phases, along with the quantity of CO_2 produced post-oxidation, will be assessed using gas chromatography GC to determine the overall process efficiency.

2. Experiment

The raw char utilized in the study is a byproduct of the pyrolysis process of scrap rubber tires conducted at a Minh Tan facility in Vietnam. Manganese nitrate solution of 50%, Colbalt Nitrate, Cerium nitrate and standard toluen solution were purchased from Xylong Ltd.

2.1. Preparation

The raw char was desiccated at 110 °C for 24 hours and subsequently ground into a fine powder using a ball mill, they are named C0. All modified char underwent temperature treatment at 800 °C within a nitrogen atmosphere. The procedure was executed as follows: degassing was performed for 30 minutes at a flow rate of 100 ml/min; subsequently, the temperature was elevated from 30 °C to 800 °C at a heating rate of 5 °C/min, followed by a maintenance period at 800 °C for 1 hour, during which the gas flow rate was adjusted to 50 ml/min. The original char that did not undergo chemical activation also underwent the above process for comparison purposes, it was named C1.

2.1.1. Char modification

Char + HCl. 7.5 grams of char was stirred in 50 ml of hot concentrated HCl for 16 hours. Then it was filtered and washed until neutral and dried at 120 °C for 12 hours, it was named C2.

Char + KOH. 2.5g of char were stirred at room temperature with 3M and 5M KOH at a velocity of 500 rpm for 3 hours. Subsequently, the char was filtered and dried it at 110 ºC for 12 hours. Afterward, it was subject to heat treatment at 800 °C per the previous procedure. Then, char was treated with 1M HCl and rinsed with distilled water until neutralized. It was conclude by drying at 110 °C for 8 hours to get the product. They was named C3 (KOH 3M) and C4 (KOH 5M).

Char + KOH + HCl. 7.5g char were soaked in 1M HCl solution and stirred at 500 rpm without heating for 3 hours. After mixing, the char was filtered and dried at 110 °C for eight hours. Next, the dried char were soaked in KOH 3M solution, stirring without heating at 500 rpm for 3 hours. Continue to filter char and dry them at 110 °C for 8 hours. Next, following the preceding steps, heat treat at 800 °C. At the end of the process, the char was washed with 1M HCl solution, then again with distilled water until pH equal 7. This sample was named C5.

2.1.2. Char/Mn-Co-CeOx preparation

A mixed metal salt solution was prepared by dissolving 3.8849 g of $Co(NO_3)_2 \cdot 6H_2O$, 0.1224 g of $Ce(NO_3)_3 \cdot 6H_2O$, and 0.531 g of a 50% $Mn(NO_3)_2$ solution in 20 mL of distilled water. To prevent hydrolysis of the metal salts during the reaction, 3–5 drops of HNO_3 were added to the mixture. Subsequently, 5 g of activated char (C5) was introduced and subjected to impregnation. The resulting material was dried at 100 °C for 8 hours and then calcined at 300 °C for 3 hours at a heating rate of 3 °C/min. The obtained catalyst was designated as Cat1. Using the same procedure with a commercial activated carbon sample, the Cat2 catalyst was prepared.

2.2. ***Characterization of Catalyst***

The specific surface area of the modified carbon samples was determined by nitrogen adsorption–desorption using a Micromeritics Gemini VII 2390 (USA). Infrared spectra were recorded on a Nicolet iS50 Fourier Transform Infrared Spectroscopy (FT-IR) spectrometer using the KBr transmittance method. Scanning Electron Microscopy (SEM) and Energy-Dispersive X-ray Spectroscopy (EDS) analyses were performed with a field-emission scanning electron microscope (JEOL JSM-7600F, USA) equipped with an Oxford Instruments X-Max 50 mm² EDS detector (UK) and a Gatan MonoCL4 cathodoluminescence (CL) probe (UK). Thermogravimetric analysis (TGA) was conducted in an inert N_2 atmosphere from room temperature to 900 °C for both untreated and treated pyrolysis char samples to monitor the thermal events occurring during high-temperature activation, using a NETZSCH TG 209F1D-0271 instrument.

2.3. Measurement of Catalytic Activity

Feed flow included toluene with a flow of nitrogen, and the overall flow rate was set at 50 mL/min. The fixed-bed reactor was used once the intake concentration of toluene achieved a constant state of 9000 ppm. A total of 0.05 grams of each catalyst (Cat1 and Cat2) was placed into the center of the 1/4-inch-diameter reactor, 0.6 meters long. Firstly, the toluene adsorption procedure was executed on MnCoCe/MC; the toluene adsorption reaction occurred instantly at room temperature. The next step was the desorption-oxidation of the previously adsorbed toluene from the catalyst MnCoCe/MC. Following saturation adsorption, the temperature of the first reactor was raised to 250 °C to initiate the desorption-oxidation process. These two processes occurred in the microreactor with a single heating reactor. An online gas chromatograph (GC) with a thermal conductivity detector (TCD) was used to measure the output flow.

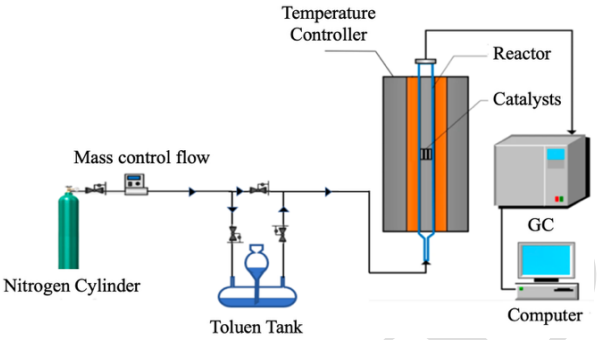

Fig 1. The scheme of reaction

The concentration of the chemicals after the reaction will be calculated using the following formulas:

Toluene conversion was evaluated as (1)

$$\eta_B = \frac{C_T^1 - C_T^2}{C_T^1} \text{x } 100 \quad (1)$$

The conversion of Toulen into CO_2 was determined as (2)

$$\gamma_{CO2} = \frac{C_{CO2.T}^2}{7(C_T^1 - C_T^2)} \text{x } 100 \quad (2)$$

In these formulas, we denote the parameters with the following meaning:

η_B: Toulen conversion (%);

C_T^1: Toluene concentration of inlet flow at a temperature T (ppm);

C_T^2: Toluene concentration of inlet flow at a temperature T (ppm).

$C_{CO2.T}^2$: CO_2 concentration of outlet flow at a temperature.

The adsorption and desorption capacity were calculated according to the formula [12]:

$$A = \frac{Q \times S_{peak} \times 10^{-6}}{60 \times 22.4 \times 10^{-3} \times m}, \text{ mmol/g} \quad (3)$$

$$S_{ads} = \sum_0^t \left[\frac{1}{2} \times \left(2C_{Max} - (C_i + C_{i+1})\right) \times \Delta t\right] \quad (4)$$

$$S_{des} = \sum_0^t \left[\frac{1}{2} \times (C_i + C_{i+1}) \times \Delta t\right] \quad (5)$$

where:

Q: Air flow rate, l/h

S_{ads}: adsorption peak area

S_{des}: desorption peak area

C_{max}: Inlet toluene concentration, ppm

C_i: toluene concentration at the time i, ppm

C_{i+1}: toluene concentration at time i+1

Δt: time interval between two measurements, minutes

m: mass of catalyst, g

60: time (minutes)

22.4: Volume of gas at standard conditions 25 °C

S_{peak}: Peak area obtained by GC

3. Results and Discussions

3.1. The Specific Surface Area

The Table 1 shows the specific surface area results of pyrolysis char and pyrolysis char after modification.

Table 1. The specific surface area of the samples

No.	Samples	S_{BET} (m^2/g)
1	Raw Char C0	52.91
2	C1 (No agent)	68.95
3	C2 (HCl)	86.03
4	C3 (KOH 3M)	118.73
5	C4 (KOH 5M)	102.94
6	C5 (HCl + KOH 3M)	142.06

The raw char (C0) sample exhibited a low surface area of 52.91 m²/g. However, following five activation methods, it can be seen that the specific surface area has improved. In combining two chemical agents, KOH and HCl, the C5 sample demonstrates the most significant specific surface area, approaching threefold that of the C0 sample (142.06 m²/g). This indicates that integrating both agents yields more effective outcomes than administering either in isolation.

In the case of sample C1, which underwent activation solely through high temperature in an inert N_2 gas

atmosphere without the introduction of chemical agents, there was an increase in the specific surface area, albeit not to a significant extent (68.95 m^2/g). Upon stirring the char in hot concentrated HCl, the specific surface area increased (86.03 m^2/g), yet it remained inferior to that achieved with KOH. This indicates that, based on the theoretical framework, KOH significantly enhances the specific surface area of pyrolysis char.

Surprisingly, the char sample activated with 5 M KOH exhibited a lower specific surface area than the one treated with 3 M KOH (102.94 < 118.73 m^2/g). According to Tan *et al*., the KOH/char ratio plays a crucial role in the development of porosity. This process is driven by the reaction between char and KOH, which produces K_2CO_3 along with the release of CO_2 and CO, contributing to pore formation and increased surface area [13]. However, Aldel *et al*. reported that an excessively high KOH/char ratio could lead to the formation of residual K_2CO_3 and metallic potassium, which are difficult to remove even after repeated washing [14]. This is supported by the EDS analysis in this study, which revealed that even with a 3 M KOH concentration, a residual potassium content of approximately 3.9% remained in the char. Such residue could potentially block the pore structures, leading to a reduction in surface area. This also explains why an overly high KOH concentration (5 M) resulted in a lower specific surface area compared to the 3 M sample. Consequently, a concentration of 3M KOH was chosen for the dual-phase treatment procedure in conjunction with HCl.

As previously indicated, sample C5 exhibits the most significant surface area; it appears that the application of HCl pre-treatment has facilitated the removal of minerals from the pyrolysis char. Subsequently, the amalgamation with KOH will significantly enhance the specific surface area. These will be discussed further in the SEM-EDS results section.

Finally, the authors will select the sample of pyrolysis rods activated by KOH 3M and HCl 1M to test the ability to treat exhaust gas by adsorption-desorption combined with oxidation.

3.2. Scanning Electron Microscopy and Energy-Dispersive X-ray Spectroscopy Results

Fig. 2 (a-g) depicts the SEM of two pyrolysis char samples before (C0) and after modification (C5). The material particles are primarily spherical or elliptical, and their sizes are consistent. However, the surface of the treated char sample is clustered and has a more even and smooth size than the untreated pyrolysis char sample, as shown in the 200k and 75k magnification pictures. It demonstrates that chemical activation eliminates the components and surrounds the char particles, causing them to be more uniformly and evenly disseminated. However, the particles were tightly gathered relatively in both samples, which is consistent with the low specific surface area results. This finding predicts that they are all kinds of char with limited adsorption ability. The char particle size is approximately 50 nm, and there is no discernible change following treatment. The particle size of pyrolysis char after treatment is significantly smaller than that of commercial activated carbon.

The produced capillary will likely be a secondary capillary between the particles; thus, the specific surface area is lower than commercial activated carbon. This demonstrates that KOH entered the char structure while impregnating, combining it with high-temperature activation to help dissolve the residual SiO_2 in the pyrolysis char. The fissures formed by the KOH stay in the same condition when the agents are washed away, resulting in increased char porosity following treatment.

Table 2. The elemental composition of raw char and char after treatment

No	Element	**C0**	**C5**	**Minerals Reduction Rate (%)**
1	C	69.8	85.8	-
2	O	14.7	8.1	44.9%
3	Si	6.4	0.8	87.5%
4	Zn	4.4	0.1	97.8%
5	S	2.1	0.4	81.0%
6	Ca	1.5	0.1	93.3%
7	Ti	1.2	0.8	33.3%
8	K	0.1	3.9	-

Table 2 presents the elemental composition derived from EDS analysis for the two char samples, C0 and C5. Post-treatment analysis reveals that the carbon content in sample C5 (85.8%) exceeds that of the original sample C0 (69.8%), This proves that the carbon content has been significantly enhanced after the activation process. The concentrations of metals, including Si, Zn, S, Ca, and Ti, exhibited a notable reduction following treatment, indicating that the interaction of HCl and KOH has effectively eliminated the impurities present in the pyrolysis char derived from tires. The elemental distribution presented in Fig. 2 illustrates this more distinctly. Post-treatment, the concentration of mineral elements exhibits a marked decrease and only appears sporadically in the mapping results. This demonstrates that applying HCl results in the dissolution of metals like Zn, Ca, and Ti. Besides, a high concentration of KOH facilitates the dissolution of Si and S.

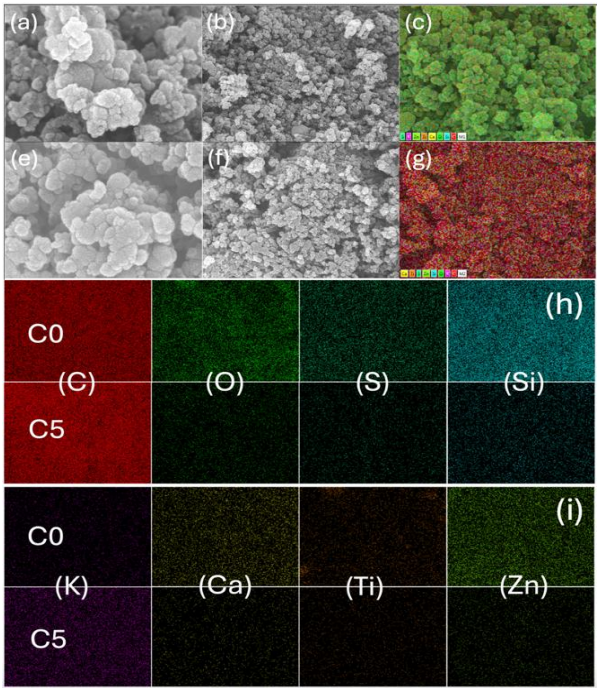

Fig 2. SEM images of the C0 char sample at (a) 200k magnification and (b) 75k magnification, with (c) elemental mapping and (h) the corresponding elemental distribution. SEM images of the C5 char sample at (e) 200k magnification and (f) 75k magnification, accompanied by (g) elemental mapping and (i) the corresponding elemental distribution

3.3. Fourier Transform Infrared Spectroscopy Results

The functional groups on the char sample before and after modification were examined using FT-IR spectroscopy (Fig. 3). The peak at 3727 cm^{-1} and 3400 cm^{-1} suggests the presence of a hydroxyl group (O-H stretching oscillations), possibly due to water adsorption from the surrounding atmosphere. The band at 1608 cm^{-1} corresponds to C=C stretching, whereas the band at 2890 cm^{-1} can be ascribed to C-H stretching oscillations [15]. The apparent double peak at 2360 cm^{-1} and 2341 cm^{-1} is characteristic of the O=C=O bond, this results from the Coblentz Society's evaluated infrared reference spectra collection, which may be due to the measurement time difference between the background and sample spectra. It can be seen that the two carbon samples, before and after modification, have similar spectral structures from the carbon bonding band onwards (from 1608 cm^{-1} to 4000 cm^{-1}), suggesting that these carbons have similar binding motifs.

The bands observed from 592–1099 cm^{-1} are typical of the silica lattice, with the band at 592 cm^{-1} thought to be the bending of the Si-O-Si bond. The band at 871 cm^{-1} represents an elongation of Si–O–Si. The asymmetric stretching of the Si-O-Si bond is attributed to the band with a rather sharp peak intensity at 1099 cm^{-1} and overtones at 1385 cm^{-1} [10]. The above bands, however, did not appear on the modified char sample, indicating that the chemical activation method strictly reduced the amount of SiO_2 in the pyrolysis char. The band at 669 cm^{-1} is characteristic of metal-oxy bonds such as ZnO. Peak 1008 cm^{-1} is assigned to the interaction of sulfide ions [16].

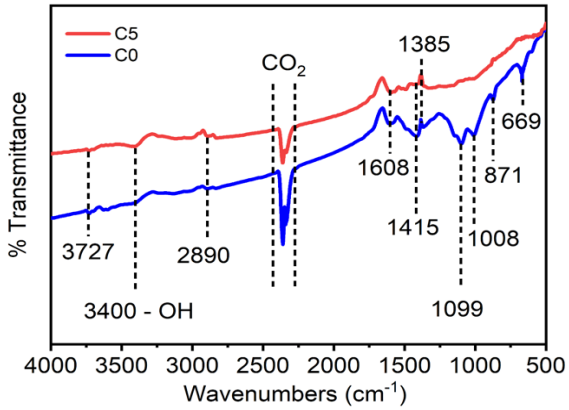

Fig 3. The FT-IR spectra of C0 and C5 samples

In addition, the spectral region between 669 and 900 cm^{-1} can be attributed to aromatic ring vibrations, suggesting the presence of residual organic compounds that have not been completely decomposed within the waste char. This observation is also consistent with the Thermogravimetric Analysis results, where the observed weight loss upon heating is associated with the degradation of certain high-molecular-weight organic compounds. Notably, this spectral region was absent in the C5 sample, indicating that the thermal treatment at 850 °C under a nitrogen atmosphere was sufficient to fully decompose the remaining organic matter.

There is also a peak at about 1400 cm^{-1} for CH_2-S asymmetric strain oscillations; refer to the Sadtler Handbook of Infrared Spectroscopy [17]. None of the above peaks are shown in the modified char sample. This proves that sulfur has been removed during activation with KOH and HCl. In summary, through FT-IR spectroscopy results, some components of pyrolysis char from tires, such as sulfur, SiO_2, and some metal oxides, have been removed by chemical agents.

3.4. Thermogravimetric Analysis Results

Fig. 4a and Fig. 4b present the TGA-DTG results for two char samples before and after KOH treatment. After heating to 900 °C for the two samples, the total mass loss is relatively similar; C0 exhibits a mass loss of 14.20%, while C5 shows a loss of 13.02%. Both samples undergo two primary stages of mass loss. The initial stage occurs between 35 °C and 150 °C, involving surface dehydration at 55.4 °C and structural dehydration at approximately 108.4 °C. The DTA results indicate that sample C0 exhibits two distinct peaks at 55.4 °C and 108.4 °C, whereas sample C5 displays a single peak at 55.4 °C. This indicates that following the chemical

activation process, the pore characteristics of the C5 sample were enhanced relative to the initial C0, resulting in increased water absorption from the air. Data indicate that the mass loss of C5 during the initial stage was 3.59%, whereas the mass loss of C0 at both temperatures was merely 2.54%.

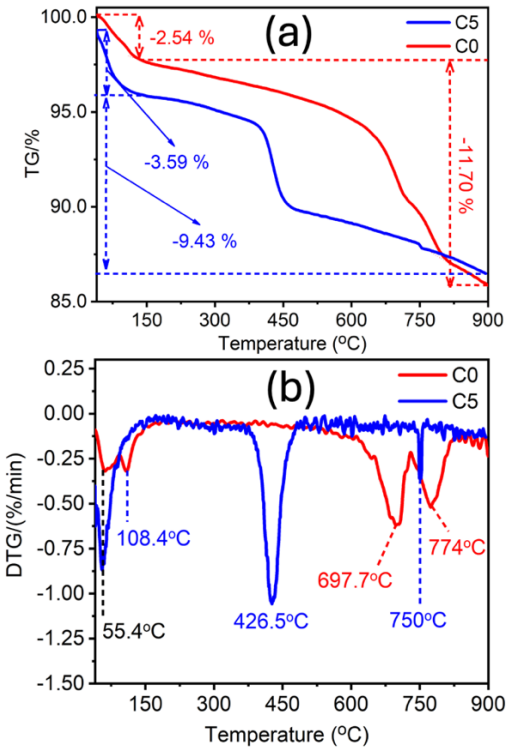

Fig 4. The TGA (a) and DTG (b) of samples

During the second stage, from 150 °C to 900 °C, the C0 char sample experienced a mass loss of up to 11.7%, with two endothermic processes occurring at the inflection points of 697.7 °C and 774 °C. In fact, ZnO, SiO_2, and CaO maintain their mass below 900 °C in a nitrogen environment. This can be attributed to mass loss from volatile organic compounds or impurities in the pyrolysis char derived from tires. The C5 char sample exhibited a distinct endothermic process at 426.5 °C, attributed to KOH, represented by the following reaction equation [18]:

$$2KOH \rightarrow K_2O + H_2O \quad (6)$$

At about 760 °C, there is still a mass a litte bit loss, which can be explained by the significant decomposition of K_2CO_3 [19]. The procedure is as follows:

$$K_2CO_3 + C \rightarrow 2KO + 3CO \quad (7)$$

In the 850 °C–900 °C region, a slight mass decrease was still observed. This may be due to the decomposition of K_2CO_3 to form [20].

This is compatible with the EDS findings, as there is only a very tiny quantity of metal impurities remaining in the sample after treatment with HCl and KOH, and the principal component with the heat shift on the TGA plot comes from KOH (remaining during the washout of the agent).

4. Catalysts Performance

Fig. 5 and Table 3 show the adsorption capacity, adsorption release, and the amount of CO_2 formed after the reaction process.

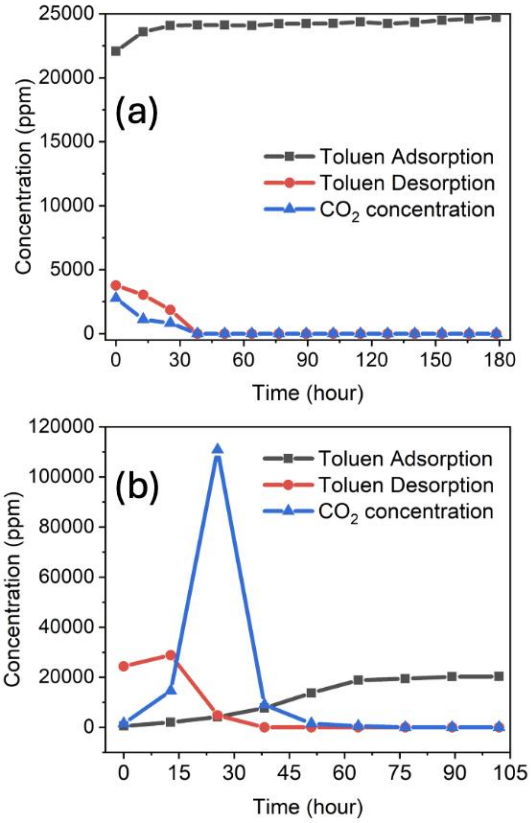

Fig. 5. The toluene adsorption, desorption, and CO_2 concentration of the sample (a) Cat1 and (b) Cat2

Tab 3. The adsorption-desorption capacity of toluene and CO_2 produced after the reaction

Catalysts	Adsorption capacity (g/g)	Desorption capacity (g/g)	CO_2 product (g/g)
C5/MnCoCe	0.2526	0.2478	0.1219
AC/MnCoCe	2.0640	0.7774	2.3248

It can be seen that the C5/MnCoCe sample has a relatively low adsorption capacity compared to the commercial activated carbon that brings on MnCoCe support. Besides, the quantity of toluene emitted during the initial phases of the process has undergone substantial oxidation, resulting in a marked decrease in its concentration. Nevertheless, the amount of

CO_2 produced is relatively minimal when assessed using the standard reaction ratio $C_6H_5\text{-}CH_3 + 9O_2 \rightarrow 7CO_2 + 4H_2O$, indicating that toluene may undergo oxidation into alternative byproducts or remain within char without undergoing complete desorption. Nonetheless, the adsorption and desorption capacities of the C5/MnCoCe sample at 250 °C are almost identical, measuring 0.2526 and 0.2478 (g/g), respectively. Consequently, one can deduce that toluene underwent oxidation, forming byproducts distinct from CO_2. This phenomenon can be attributed to the extensive surface area and the more intricate pore architecture of commercial activated carbon. Activated carbon is frequently subjected to specialized treatments to improve its adsorption ability.

Indeed, the commercial activated char exhibited a specific surface area of 888.5 m²/g. Upon loading with MnCoCe mixed metal oxides, this value decreased to 537 m²/g, indicating that the metal oxide particles had penetrated into the pore structure, thereby reducing the specific surface area. A similar trend is expected for the chemically activated char, whose surface area reached only 142.06 m²/g, approximately six times lower than that of the commercial sample. However, since this study aims to develop a dual-function material capable of both adsorbing and catalytically oxidizing toluene, a certain degree of surface area reduction following metal oxide impregnation is to be expected. Therefore, the key focus should be placed on maximizing the surface area of the waste-derived char during the activation stage.

5. Conclusions

This study conducted a series of chemical activation methods on char derived from the pyrolysis of waste tires, using two main activating agents: KOH and HCl. Among them, the char sample activated with 3 M KOH and 1 M HCl exhibited the highest specific surface area, nearly three times greater than that of the raw char. The SEM-EDS and FT-IR analyses indicated that the mineral constituents in the original pyrolysis char, which influence the char's attributes post-modification, had been nearly completely addressed. Furthermore, the TGA-DSC data indicated that the mass loss of the char resulted from the degradation of high molecular weight organic compounds and residual KOH remaining after the modification procedure, without any structural collapse taking place. This study has delineated a definitive course for the alteration of char resulting from the tire pyrolysis process at the Minh Tan Vietnam facility. To enhance the specific surface area, it is probable that the modification conditions may need to be adjusted in further research. For instance, concurrent heat treatment with char and KOH may be performed, or the duration of mixing with chemical agents may be extended.

Acknowledgement

This research has been supported by the RoHan Project funded by the German Academic Exchange Service (DAAD, No. 57315854) and the Federal Ministry for Economic Cooperation and Development (BMZ) inside the framework “SDG Bilateral Graduate School programme”.

References

[1] N. Gao, F. Wang, C. Quan, L. Santamaria, G. Lopez, and P. T. Williams, Tire pyrolysis char: processes, properties, upgrading and applications, Progress in Energy and Combustion Science, vol. 93, Nov. 2022, Art. no. 101022. https://doi.org/10.1016/j.pecs.2022.101022

[2] A. Donatelli, P. Iovane, and A. Molino, High energy syngas production by waste tyres steam gasification in a rotary kiln pilot plant. Experimental and numerical investigations, Fuel, vol. 89, iss. 10, pp. 2721–2728, Oct. 2010. http://dx.doi.org/10.1016/j.fuel.2010.03.040

[3] S. Doja, L. K. Pillari, and L. Bichler, Processing and activation of tire-derived char: a review, Renewable and Sustainable Energy Reviews, vol. 155, Mar. 2022, Art. no. 111860. https://doi.org/10.1016/j.rser.2021.111860

[4] M. Wu, Q. Guo, and G. Fu, Preparation and characteristics of medicinal activated carbon powders by CO_2 activation of peanut shells, Powder Technology, vol. 247, pp. 188–196, Oct. 2013. https://doi.org/10.1016/j.powtec.2013.07.013

[5] E. M. Mistar, T. Alfatah, and M. D. Supardan, Synthesis and characterization of activated carbon from Bambusa vulgaris striata using two-step KOH activation, Journal of Materials Research and Technology, vol. 9, no. 3, pp. 6278–6286, May–Jun. 2020. https://doi.org/10.1016/j.jmrt.2020.03.041

[6] O. Oginni, K. Singh, G. Oporto, B. Dawson-Andoh, L. McDonald, and E. Sabolsky, Influence of one-step and two-step KOH activation on activated carbon characteristics, Bioresource Technology Reports, vol. 7, Jun. 2019, Art. no. 100266. https://doi.org/10.1016/j.biteb.2019.100266

[7] A. A. Nuhu, I. C. P. Omali, and C. O. Clifford, Equilibrium adsorption studies of methylene blue onto caesalpinia pulcherrima husk-based activated carbon, Chemical Science International Journal, vol. 26, iss. 3, pp. 1–11, Apr. 2019. https://doi.org/10.9734/CSJI/2019/v26i330096

[8] S. Lv, C. Li, J. Mi, and H. Meng, A functional activated carbon for efficient adsorption of phenol derived from pyrolysis of rice husk, KOH-activation and EDTA-4Na-modification, Applied Surface Science, vol. 510, Apr. 2020, Art. no. 145425. https://doi.org/10.1016/j.apsusc.2020.145425

[9] J.-H. Lin and S.-B. Wang, An effective route to transform scrap tire carbons into highly-pure activated carbons with a high adsorption capacity of ethylene blue through thermal and chemical treatments, Environmental Technology and Innovation, vol. 8, pp. 17–27, Nov. 2017. https://doi.org/10.1016/j.eti.2017.03.004

[10] R. Shilpa, R. Kumar, and A. Sharma, Morphologically tailored activated carbon derived from waste tires as high-performance anode for Li-ion battery, Journal of Applied Electrochemistry, vol. 48, no. 1, pp. 1–13, 2018. https://doi.org/10.1007/s10800-017-1129-3

[11] M. T. Le, T. T. Nguyen, P. T. M. Pham, E. Bruneel, and I. Van Driessche, Activated MnO_2-Co_3O_4-CeO_2 catalysts for the treatment of CO at room temperature, Applied Catalysis A: General, vol. 480, pp. 34–41, Jun. 2014. https://doi.org/10.1016/j.apcata.2014.04.034

[12] P. L. E. Cloirec, Nanoporous adsorbents for air pollutant removal, in Nanoporous Materials: Science and Engineering, Chapter 25, pp. 772–811, Nov. 2004. https://doi.org/10.1142/9781860946561_0025

[13] I. A. W. Tan, A. L. Ahmad, and B. H. Hameed, Preparation of activated carbon from coconut husk: Optimization study on removal of 2, 4, 6-trichlorophenol using response surface methodology, Journal of Hazardous Materials, vol. 153, iss. 1–2, pp. 709–717, May 2008. https://doi.org/10.1016/j.jhazmat.2007.09.014

[14] A.-N. A. El-Hendawy, An insight into the KOH activation mechanism through the production of microporous activated carbon for the removal of Pb^{2+} cations, Applied Surface Science, vol. 255, no. 6, pp. 3723–3730, 2009. https://doi.org/10.1016/j.apsusc.2008.10.034

[15] R. Mis-Fernandez, J. A. Azamar-Barrios, and C. R. Rios-Soberanis, Characterization of the powder obtained from wasted tires reduced by pyrolysis and thermal shock process, Journal of Applied Research and Technology, vol. 6, no. 2, pp. 95–104, Aug. 2008. https://doi.org/10.22201/icat.16656423.2008.6.02.516

[16] B. S. Rema Devi, R. Raveendran, and A. V Vaidyan, Synthesis and characterization of Mn^{2+}-doped ZnS nanoparticles, Pramana, vol. 68, no. 4, pp. 679–687, May 2007. https://doi.org/10.1007/s12043-007-0068-7

[17] S. Ouyang, D. Xiong, Y. Li, L. Zou, and J. Chen, Pyrolysis of scrap tyres pretreated by waste coal tar, Carbon Resources Conversion, vol. 1, iss. 3, pp. 218–227, 2018. https://doi.org/10.1016/j.crcon.2018.07.003

[18] Y. Huang, E. Ma, and G. Zhao, Thermal and structure analysis on reaction mechanisms during the preparation of activated carbon fibers by KOH activation from liquefied wood-based fibers, Industrial Crops and Products, vol. 69, pp. 447–455, Jul. 2015. https://doi.org/10.1016/j.indcrop.2015.03.002

[19] J. Wang and S. Kaskel, KOH activation of carbon-based materials for energy storage, Journal of Materials Chemistry, vol. 22, iss. 45, pp. 23710–23725, 2012. https://doi.org/10.1039/c2jm34066f

[20] R. L. Lehman, J. S. Gentry, and N. G. Glumac, Thermal stability of potassium carbonate near its melting point, Thermochimica Acta, vol. 316, iss. 1, pp. 1–9, May 1998. https://doi.org/10.1016/S0040-6031(98)00289-5